JOURNAL OF GUIDANCE, CONTROL, AND DYNAMICS
Vol. 26, No. 4, July–August 2003

Nonlinear Statistical Approach for Aeroelastic Response Prediction

Cristina Adela Popescu* and Yau Shu Wong†
University of Alberta, Edmonton, Alberta T6G 2G1, Canada

Aging aircraft and combat aircraft that carry heavy external stores potentially face problems arising from nonlinearities in structure. An expert data mining system is proposed that is capable of predicting the asymptotic behavior of an aeroelastic system with structural nonlinearities represented by polynomial restoring forces or freeplay models. The input is represented only by a limited set of transient data. The output provides a long-term nonlinear aeroelastic response, and the prediction is made when certain rule-based reasoning conditions are satisfied. An attractive feature of this new approach is that no information about the system parameters is needed. In the prediction module, we propose two methods, based on nonlinear time series models and the unscented Kalman filter. To our knowledge, these approaches have not been reported so far for predicting the long-term nonlinear aeroelastic responses. Compared with the classical extended Kalman filter, the unscented filter does not require differentiability and can be applied to nonlinear aeroelastic models with freeplay and hysteresis. The performances of the expert data mining system are demonstrated for simulated data and wind-tunnel experimental aeroelastic data resulting from a two-degree-of-freedom airfoil oscillating in pitch and plunge.

Nomenclature

$E[x\|y]$	=	conditional expectation of x with respect to y
m	=	maximum regression order for the estimation of a time series model
N	=	number of observations
$\bar{P}_n$	=	$E[\{x_n - \bar{x}_n\}\{x_n - \bar{x}_n\}^T \| y_1, \ldots, y_n]$
$\hat{P}_{n+1}$	=	$E[\{x_{n+1} - \hat{x}_{n+1}\}\{x_{n+1} - \hat{x}_{n+1}\}^T \| y_1, \ldots, y_n]$
$\hat{P}_{xy(n+1)}$	=	$E[\{x_{n+1} - \hat{x}_{n+1}\}\{y_{n+1} - \hat{y}_{n+1}\}^T \| y_1, \ldots, y_n]$
$\hat{P}_{v(n+1)}$	=	$E[\nu_{n+1}\nu_{n+1}^T \| y_1, \ldots, y_n]$
q	=	dimension of the process noise v
s	=	dimension of the state space
X_n	=	current observations of the given time series
x_n	=	state at the discrete time n
$\bar{x}_n$	=	$E[x_n \| y_1, \ldots, y_n]$
$\hat{x}_{n+1}$	=	$E[x_{n+1} \| y_1, y_2, \ldots, y_n]$
$\bar{\mathbf{x}}_n^a$	=	$[\bar{x}_n, 0]^T$
y_n	=	observation at the discrete time n
ν_{n+1}	=	$y_{n+1} - \hat{y}_{n+1}$

Introduction

AN understanding of the nonlinear aeroelastic response is a crucial problem for the aerospace community because the complex aeroelastic phenomenon plays an important role in the safe design of an aircraft. The classical linear theory is not appropriate for studying limit-cycle oscillations (LCOs), and it may lead to inaccurate results for predicting the flutter boundaries.[1] In a nonlinear formulation, the aeroelastic problem has been studied by many researchers via mathematical analysis and numerical simulations. Several mathematical models based on nonlinear systems of ordinary differential equations (ODEs), which can be expressed in state-space form, have been employed to study the LCOs and flutter for various types of airfoils and nonlinearities.[2–4] In the cited papers, the nonlinear ODE system is studied using numerical approaches based on finite difference methods, the Runge–Kutta time-integrating scheme, or the describing function technique. For nonlinear control of a prototypical wing section with a torsional nonlinearity, Ko et al.[5] also consider a model based on an ODE system that can be expressed in state-space form. They investigate a model with polynomial nonlinearities, and Lie algebraic methods are employed for feedback controllers. The results are validated by the experiments performed at Texas A&M University.[6]

In practice, such as with the ground vibration test and the actual flight test, only the dynamic response corresponding to a given excitation is recorded. Hence, it is desirable to develop a technique such that one could predict the LCO and other complex aeroelastic phenomena from the dynamic response only. A possible solution is to use a neural-network approach.[7] The goal of this paper is to present a new methodology based on modern data processing techniques, in which an expert data mining system (EDMS) is developed. The basic structure of an EDMS is illustrated in Fig. 1. The EDMS is especially designed to deal with aeroelastic data with structural nonlinearities. We propose two new approaches for the long-term prediction of the aeroelastic response, namely the nonlinear time series models and the unscented filter[8] (UF). Compared with a neural-network approach, the proposed nonlinear time series models are computationally efficient, and they require simple training algorithms. In addition, the UF method can take advantage of information about the mathematical models associated with the experimental data, and thus it can provide more accurate predictions.

Given a time series $X = [x_1, x_2, \ldots, x_n]$, which contains a limited number of transient observations, we want to predict the subsequent values $[x_{n+1}, x_{n+2}, \ldots]$. In a classical approach, linear time series models or the Kalman filter are commonly used to perform one-step-ahead predictions or short-term predictions. The main advantage of the two nonlinear approaches proposed in this paper is the capability of making not only short-term predictions, but also accurate long-term predictions. The classification rules of the EDMS inference engine are based on these long-term predictions. If the results obtained with two different approaches agree, the final output of the EDMS gives the asymptotic characterization of the system (such as LCO or damped or divergent oscillations) together with the predicted nonlinear motions.

Linear time series models, such as autoregressive moving average (ARMA)[9,10] or autoregressive moving average with exogenous variable (ARMAX)[11] models, are frequently used for system identification of aeroelastic system and flutter prediction. Because the

Presented as Paper 2002-1281 at the Structures, Structural Dynamics and Materials Conference, Denver, April 2002; received 22 April 2002; revision received 13 March 2003; accepted for publication 8 April 2003.

*Ph.D. Candidate, Department of Mathematical and Statistical Sciences, 632 Central Academic Building. Student Member AIAA.

†Professor, Department of Mathematical and Statistical Sciences, 632 Central Academic Building.

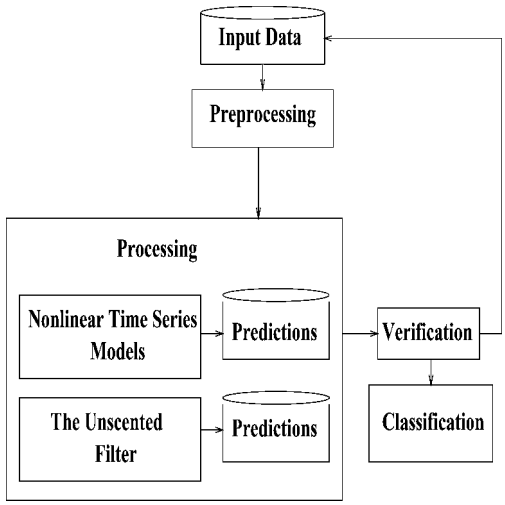

Fig. 1 Expert data mining system.

nonlinearities in the aerodynamics or the structure of an aircraft can critically affect the aeroelastic behavior, it is, therefore, desirable to develop nonlinear models. Another important consideration in developing the EDMS is the capability to handle input data corrupted with noise. The performances of ARMA and ARMAX models are known to be very sensitive to the measurement errors.[12] Tests carried out at the noise levels of 5, 10, 15, and 20% found that the mean flutter prediction using ARMA-based methods was acceptable only for the case with 5% noise level. To overcome this difficulty, wavelet filters have been implemented in the preprocessing module of the EDMS. Consequently, the parameter estimating procedures can be applied to the filtered signal instead of the original noisy data.

Kalman estimators have a long history in the study of aeroelastic phenomena (see Ref. 13). The extended Kalman filter (EKF) is often applied as a real-time parameter identifier (see Ref. 14). However, the EKF can not be applied to nondifferentiable nonlinearities such as those encountered in freeplay or hysteresis models. In the proposed EDMS, we consider the UF.[15] Its performance is comparable to the EKF,[15] but the UF does not require the calculation of any Jacobians. Thus, the UF method is capable of dealing with continuous nondifferentiable nonlinearities, and it is computationally efficient.

Preprocessing

Generally speaking, all real data are contaminated by noise. However, the noise effect may vary. For instance, the noise content from a typical ground test is usually small, and the majority is caused by the measurement noise. On the other hand, in a flight flutter test, the amount of noise corruption due to turbulence is often significant. Because an important difficulty in using nonlinear time series models is due to their sensitivity to noise, it is important to reduce the noise effects. In this study, we apply a wavelet filtering,[16] which mainly uses a transform-based thresholding, working in three steps.

1) Transform the noisy data into an orthogonal domain.

2) Apply soft or hard thresholding to the resulting coefficients, thereby suppressing those coefficients smaller than a certain amplitude.

3) Transform back into the original domain.

The wavelet transform is based on a multiresolution analysis.[17] By multiresolution, a wavelet transform can be organized as a ladder of component stages, each one involving simply the application of digital filtering to certain discrete time "signals." Consequently, this leads to a fast and efficient orthogonal transform of $\mathcal{O}(N)$. Our C++ implementation of the wavelets filters is based on the MATLAB® programs of WAVELAB (available online at http://www-stat.stanford.edu/wavelab/ [cited 21 May 2003]).

Denoising using hard and soft thresholding and orthogonal maximally decimated wavelet transforms can cause certain visual artifacts, some of them due to the lack of translation invariance of the wavelet basis. To overcome these difficulties, we apply translation invariant transformations[16]: The noisy signal is shifted, then denoised with wavelet thresholding, and finally unshifted. The implementation of this method over the range of all circulant shifts is of $\mathcal{O}(N \log_2 N)$.

In addition to the denoising step, the input data are transformed to the interval $[-1, 1]$, and we work with the mean deleted time series. Moreover, as part of the preprocessing module, we apply standard linearity, stationarity, and Gaussian tests to the input data.[18]

Nonlinear Time Series Models

Two nonlinear time series models, namely, the amplitude-dependent exponential autoregressive models (EXPAR)[19] and the self-exciting autoregressive models (SETAR),[18] are being considered. Because the EDMS is designed to deal with nonstationary data that exhibit complex nonlinear dynamics, we prefer nonlinear models. The EXPAR models are suitable for polynomial structural nonlinearities, and the SETAR models include the threshold structure specific to freeplay or hysteresis. The performance assessment of the EXPAR and SETAR models is based on the study of residuals.[18]

Amplitude-Dependent EXPAR

The EXPAR models incorporate both the amplitude-dependent frequency and the limit-cycle behavior. The basic form of an EXPAR model of order p is given by

$$X_n = \left(\Phi_1 + \pi_1 e^{-\gamma X_{n-1}^2}\right) X_{n-1} + \cdots + \left(\Phi_p + \pi_p e^{-\gamma X_{n-1}^2}\right) X_{n-p} + e_n \tag{1}$$

where $\Phi_i, \pi_i, i = 1, \ldots p$, and γ are constants and e_n is a discrete Gaussian white noise process. Such a model implies that X_n is a symmetric process, although X_n is not constrained to being Gaussian.

If we ignore the white noise input, it has been shown[20] that the necessary conditions for the solutions of Eq. (1) to exhibit a limit-cycle behavior are 1) the roots of $\lambda^p - \Phi_1\lambda^{p-1} - \cdots - \Phi_p = 0$ lie inside the unit circle, 2) the roots of $\lambda^p - (\Phi_1 + \pi_1)\lambda^{p-1} - \cdots - (\Phi_p + \pi_p) = 0$ do not lie inside the unit circle, and 3) there is no nonzero singular point, or all nonzero singular points are unstable.

These conditions replace the usual stability conditions for the ARMA models, and they can be used to generalize the approach in Ref. 10 for finding the flutter margin.

For complex dynamic predictions, the EXPAR model (1) can be extended[20] to the following form:

$$X_n = \left(\Phi_1 + f_1(X_{n-1})e^{-\gamma X_{n-1}^2}\right) X_{n-1} + \cdots + \left(\Phi_p + f_p(X_{n-1})e^{-\gamma X_{n-1}^2}\right) X_{n-p} + e_n \tag{2}$$

where $f_i(X_{n-1})e^{-X_{n-1}^2}, i = 1, \ldots, p$, are Hermite-type polynomials:

$$f_i(X_{n-1}) = \pi_0^{(i)} + \pi_1^{(i)} X_{n-1} + \cdots + \pi_{r_i}^{(i)} X_{n-1}^{r_i} \tag{3}$$

The model given in Eq. (2) admits a more sophisticated nonlinear dynamics. For example, if the order r_i of the polynomials $f_i(X_{n-1})$ are odd, then X_n is not constrained to being a symmetric process.

We now briefly present an efficient procedure for estimating the coefficients of the EXPAR model (2). In general, the estimation of the order p and the coefficients $\{\gamma, (\Phi_i, \pi_j^{(i)}), j = 0, \ldots, r_i, i = 1, \ldots, p\}$ require a nonlinear optimization procedure. However, this optimization problem can be reduced to the fitting of a linear regression.[19] For $n = m + 1, \ldots, N$, we rewrite Eq. (2) as

$$X^{(N)} = A\beta + \boldsymbol{e} \tag{4}$$

where

$$\beta = \left[\Phi_1, \pi_0^{(1)}, \ldots, \pi_{r_1}^{(1)}, \ldots, \Phi_p, \pi_0^{(p)}, \ldots, \pi_{r_p}^{(p)}\right]^T \tag{5}$$

$$A = \Big[X^{(N-1)}, Y_0^{(N-1)}, \ldots, Y_{r_1}^{(N-1)}, \ldots, X^{(N-p)}, Y_0^{(N-p)}, \ldots, Y_{r_p}^{(N-p)} \Big] \tag{6}$$

$$\boldsymbol{e} = [e_N, e_{N-1}, \ldots, e_{m+1}]^T \tag{7}$$

Here,

$$X^{(n)} = [X_n, X_{n-1}, \ldots, X_{n-(N-m-1)}]^T \tag{8}$$

$$Y_i^{(n)} = \Big[X_n e^{-\gamma X_{N-1}^2} X_{N-1}^i, X_{n-1} e^{-\gamma X_{N-2}^2} X_{N-2}^i, \ldots, X_{n-(N-m-1)} e^{-\gamma X_m^2} X_m^i \Big]^T \tag{9}$$

The parameter γ is selected from a grid in a range such that $e^{-\gamma X_{n-1}^2}$ is different from both 0 and 1 for most values of X_{n-1}. For each value of γ, β is estimated using a singular value decomposition in the normal equations,

$$A\beta = X^{(N)} \tag{10}$$

The choice of the maximum order m is subjective, and it depends on the sample size. The order p of the fitted model is determined using the Akaike's information criterion (AIC) for the nonlinear time series,[19] that is,

$$\mathrm{AIC}(p) = (N-m)\log\hat{\sigma}_p^2 + 2\left(2p + \sum_{i=1}^{p} r_i + 1\right) \tag{11}$$

where $\hat{\sigma}_p^2$ is the least-square estimate of the residual variance of the model. The last term in Eq. (11) represents the double of the number of estimated parameters in the model, including the fitted mean. For each γ, the fitted models are compared again using the AIC, and the model with the smallest AIC is chosen.

The complexity of the singular value decomposition method is proportional with

$$(N-m)\left(2p + \sum_{i=1}^{p} r_i\right)^2 + \left(2p + \sum_{i=1}^{p} r_i\right)^3 \tag{12}$$

Thus, the estimation method is computationally efficient for models of reasonably large order.

SETAR

The essential idea underlying the SETAR models is a piecewise linearization of the nonlinear models over the state space with the introduction of thresholds.

Let $\{t_0, t_1, \ldots, t_l\}$ denote the thresholds, that is, a linearly ordered subset of real numbers, such that $t_0 < t_1 < \cdots < t_l$, where $t_0 = -\infty$ and $t_l = +\infty$. A self-exciting threshold autoregressive model of order $(l; p, \ldots, p)$ or SETAR $(l; p, \ldots, p)$, where p is repeated l times, is a univariate time series $\{X_n\}$ of the form

$$X_n = a_0^{(j)} + \sum_{i=1}^{p} a_i^{(j)} X_{n-i} + e_n^{(j)} \tag{13}$$

conditional on $X_{n-d} \in T_j$, $j = 1, 2, \ldots l$, where $T_j = (t_{j-1}, t_j]$, d is a fixed integer belonging to $\{1, 2, \ldots, p\}$, and $\{e_n^{(j)}\}$ is a Gaussian uncorrelated white noise sequence. If for $j = 1, 2, \ldots, l$, we have $a_i^{(j)} = 0$ for $i = p_j + 1, p_j + 2, \ldots, p$, then $\{X_n\}$ is known as a SETAR$(l; p_1, p_2, \ldots, p_l)$ model. Hence, a SETAR $(1, p)$ model is equivalent to a linear autoregressive (AR) model of order p.

We now briefly describe the parameter estimation[21] for a SETAR$(2; p_1, p_2)$ model. First, let d and m be predefined, where m is the maximum regression order of the two linear AR models, and let n_0 be the maximum of d and m. The choice of m is subjective and usually depends on the sample size. To estimate the threshold t_1, we try some of the sample quantiles, for example, $\{Q_{0.30}, Q_{0.40}, Q_{0.50}, Q_{0.60}, Q_{0.70}\}$, where by definition, for any $0 < q < 1$, exactly $100q\%$ of the data are less than Q_q. For each choice of t_1, the data set is rearranged into two subsets, and two subsystems of linear AR equations are set up. The first subset contains the observations less than or equal to t_1, and the second subset contains the observations greater than t_1. The coefficients are then estimated using a singular value decomposition for each of the corresponding matrices. For each value of t_1 and d, we apply the Akaike's information criterion to determine p_1 and p_2, the orders of the two linear ARs.

A combination of a SETAR model with EXPAR models is further developed for an aeroelastic model with freeplay. To construct this model, we replaced the linear AR models in Eq. (13) with the EXPAR models given by Eq. (2). The parameters are estimated combining the algorithms for EXPAR and SETAR models. The most difficult task for these models is to find the thresholds and the delay parameter d. In EDMS, we use mainly exploratory data analysis (the methods presented in Ref. 18, chapters 7.2.3 and 7.2.9).

UF

A typical EKF linearizes all nonlinear models using Jacobians, so that the traditional Kalman filter (KF) equations can be applied. However, in practice, linearization can produce highly unstable filters if the local linearity is violated. In addition, the functions must be at least continuous differentiable, and the derivation of the Jacobian matrices is usually expensive and nontrivial in most applications.

In this paper, we consider the UF,[8,15] which applies the recursive linear estimator structure of the KF, but it eliminates the EKFs linearization assumptions. Because no Jacobian matrices are needed, it only requires continuity, but not differentiability. (This is of obvious importance for a freeplay model.) In contrast to first-order accuracy of the EKF, the UF is capable of accurately capturing the true posterior mean and covariance up to the third order. For general state-space problems, the EKF and the UF have an equal computational complexity $\mathcal{O}(s^3)$, where s is the dimension of the state space.

Consider a general nonlinear discrete-time system

$$x_{n+1} = f(x_n, u_{n+1}, v_{n+1}) \tag{14}$$

$$y_{n+1} = h(x_{n+1}, u_{n+1}) + w_{n+1} \tag{15}$$

where $f(\cdot,\cdot,\cdot)$ is the process model, $h(\cdot,\cdot)$ is the observation model, v_{n+1} and w_n are Gaussian noise vectors from uncorrelated white sequences, and u_{n+1} is the input vector. The classical Kalman update equations at time $n+1$ are

$$\bar{x}_{n+1} = \hat{x}_{n+1} + G_{n+1} v_{n+1} \tag{16}$$

$$\bar{P}_{n+1} = \hat{P}_{n+1} - G_{n+1} \hat{P}_{v(n+1)} G_{n+1}^T \tag{17}$$

Here, v_{n+1} is the innovation, and G_{n+1} is the Kalman gain:

$$G_{n+1} = \hat{P}_{xy(n+1)} \hat{P}_{v(n+1)}^{-1} \tag{18}$$

With this updating scheme, the main problem remains the optimal prediction of $\hat{x}_{n+1}$ and $\hat{P}_{n+1}$. For nonlinear models, both the EKF and the UF approximate these quantities. To state the UF equations, let define an augmented vector $\boldsymbol{x}_n^a$, where $\boldsymbol{x}_n^a = (x_n, v_{n+1})^T$. For the UF filtering algorithm, the following steps must be carried out.[15]

1) Compute a set of translated sigma points from $\bar{P}_n^a$, the covariance matrix of $\bar{\boldsymbol{x}}_n^a$:

$$\sigma_i^a(n|n) \leftarrow \text{ rows or columns from } \pm\left[(s+q+\gamma)\bar{P}_n^a\right]^{\frac{1}{2}}$$

$$\chi_0(n|n) = \bar{\boldsymbol{x}}_n^a,\ \chi_i(n|n) = \sigma_i^a(n|n) + \bar{\boldsymbol{x}}_n^a \tag{19}$$

2) Evaluate $\chi_i(n+1|n) = f(\chi_i(n|n), u_{n+1})$, for $i = 0, \ldots, 2(s+q)$.

3) Compute the predicted mean as

$$\hat{x}_{n+1} = \frac{1}{s+q+\gamma}\left\{\gamma\chi_0(n+1|n) + \frac{1}{2}\sum_{i=1}^{2(s+q)} \chi_i(n+1|n)\right\} \tag{20}$$

4) Compute the predicted covariance as

$$\hat{P}_{n+1} = \frac{1}{s+q+\gamma}\left\{\gamma[\chi_0(n+1|n) - \hat{x}_{n+1}][\chi_0(n+1|n) - \hat{x}_{n+1}]^T + \frac{1}{2}\sum_{i=1}^{2(s+q)}[\chi_i(n+1|n) - \hat{x}_{n+1}][\chi_i(n+1|n) - \hat{x}_{n+1}]^T\right\} \quad (21)$$

5) Predict the expected observation $\hat{y}_{n+1}$ and the innovation covariance $\hat{P}_{v(n+1)}$ using similar formulas and $Y_i(n+1|n) = h[\chi_i(n+1|n), u_{n+1}]$.

6) Predict the cross-correlation matrix $\hat{P}_{xy(n+1)}$ using $Y_i(n+1|n)$ and $\chi_i(n+1|n)$.

To minimize the mean-squared error up to the third order, the parameter γ must be chosen equal to $3 - s$.

To apply the UF for simulated and experimental aeroelastic data, a mathematical model expressed by a nonlinear ODE system[2,5] is employed:

$$X'(t) = AX(t) + F[X(t)] \quad (22)$$

Here A is a matrix, F is a nonlinear function, X is the state vector representing the plunging deflection ξ, the pitch angle about the elastic axis α, and their derivatives ξ' and α'. We consider functions F that can be expressed mathematically by polynomials in pitch or plunge, or in a freeplay case, F is a continuous piecewise linear function. Only two variables, the plunging deflection and the pitch angle, can be measured in practice. Hidden variables correspond to ξ', α', and the system parameters. When Eq. (22) and a fourth order Runge–Kutta integration scheme are used, the problem can be reformulated in a discrete-time state-space form:

$$\begin{bmatrix} x_{n+1} \\ a_{n+1} \end{bmatrix} = \begin{bmatrix} f(a_n, x_n) \\ a_n \end{bmatrix} + v_{n+1} \quad (23)$$

$$y_{n+1} = \begin{bmatrix} 1 & 0 & 0 & \dots & 0 \\ 0 & 1 & 0 & \dots & 0 \end{bmatrix} \begin{bmatrix} x_{n+1} \\ a_{n+1} \end{bmatrix} + w_{n+1} \quad (24)$$

where $x_n = [\xi_n, \alpha_n, \xi', \alpha']^T$, a_n is a vector formed with the system parameters (the elements of the matrix A and the coefficients of the polynomial or piecewise linear function F), $y_n = [\xi_n, \alpha_n]^T$, and f is a nonlinear continuous function corresponding to the Runge–Kutta scheme for Eq. (22). The filter simultaneously produces estimations for the system parameters and for ξ, α, ξ' and α'.

After the application of the filter using the transient noisy observations, the predictor is applied to provide the asymptotic system behavior. The parameters are chosen to be the last values estimated using the filter. For the UF predictor, the corresponding state-space formulation is given by

$$x_{n+1} = f(\boldsymbol{a}, x_n) + v_{n+1} \quad (25)$$

$$y_{n+1} = \begin{bmatrix} 1 & 0 & 0 & 0 \\ 0 & 1 & 0 & 0 \end{bmatrix} x_{n+1} + w_{n+1} \quad (26)$$

where $\boldsymbol{a}$ is a constant vector containing the estimated values of the parameters. Here the dimension of the state space is four, and the dimension of the observation space remains two.

A theoretical study of the estimation error for the nonlinear system (24) and (23) is difficult, especially in a freeplay case, when the function f is not differentiable. Because the method is mainly employed for predictions, when we run the filter, we check numerically the convergence of the estimations of the parameters. We also study the accuracy of the predicted values for ξ and α.

Verification

To measure the accuracy of the long-term prediction, the available input data are divided into two subsets: the training set and the test set. The training set is used to estimate the parameters of the models to be used for predictions. The test set is used to check the accuracy of the predictions. The performance assessment is based on the study of the residuals on both the training and the test sets. An advantage of this method is that it emphasizes the predictive aspect of the model selection.

Two different methods, the nonlinear time series models and the UF, are being proposed for prediction in the EDMS. Hence, a diagnostic check for each prediction can be performed by comparing the results of these two different approaches. Other prediction methods, such as a neural-network approach,[7] can be easily incorporated to enhance the capability of the proposed EDMS.

A typical expert system consists of two core components, namely, the knowledge base and the reasoning engine. In the present EDMS, the knowledge base involves data analysis reported in the preceding section, in which the nonlinear time series models and the UF method are used to process the input data and to provide long-term predictions. Before an output and conclusions are presented, the information obtained from the knowledge base must be reasoned, and certain rules have to be satisfied. In our system, a simple rule is applied, namely, the long-term predictions and their classification as LCO or stable or unstable oscillations are given as the system output provided two solutions from two different approaches in the processing step agree.

Applications

We have implemented the preprocessing, prediction, and verification steps using a C++-based program. To demonstrate the effectiveness of the developed EDMS, we report long term predictions using simulated and experimental aeroelastic data. With the nonlinear time series approach, for each new set of data we need to estimate the parameters. When only the initial conditions are different, to use the same parameter estimation for several sets of data, the expectation maximization algorithm can be used in conjunction with the UF.[22] However, note that the two approaches presented here are computationally attractive and that they can be considered for real-time applications.

In Figs. 2–7, the x axis displays the nondimensional discrete time and the y axis the pitch angle in radians or the nondimensional plunging deflection.

Simulated Data

The input data is generated from a mathematical model that simulates a two-degree-of-freedom airfoil oscillating in pitch and plunge[2]

$$\xi'' + x_\alpha\alpha'' + 2\zeta_\xi(\tilde{\omega}/U^*)\xi' + (\tilde{\omega}/U^*)^2 G(\xi) = -(1/\pi\mu)C_L(\tau) \quad (27)$$

$$\left(x_\alpha/r_\alpha^2\right)\xi'' + \alpha'' + 2\left(\zeta_\alpha/U^*\right)\alpha' + (1/U^{*2})M(\alpha) = \left(2/\pi\mu r_\alpha^2\right)C_M(\tau) \quad (28)$$

where $G(\xi)$ and $M(\alpha)$ are the nonlinear plunge and pitch stiffness terms and $C_L(\tau)$ and $C_M(\tau)$ are the lift and pitching moment coefficients. The integro–differential system can be reformulated[2] as an ODE system similar to Eq. (22). The structural nonlinearities are represented by the the nonlinear stiffness terms $G(\xi)$ and $M(\alpha)$.

The nonlinear aeroelastic system is solved numerically using a fourth-order Runge–Kutta time-integration scheme. To investigate more realistic test cases, extra white noise with the signal-to-noise ratio (SNR) 5 is added to the simulated data. A typical input data consists of the 150–400 transient observations. The majority of these data are used as a training set, and the remaining data form the test set. We illustrate here the freeplay case with system parameters chosen so that the aeroelastic responses correspond to LCOs and unstable oscillations. In Fig. 2, we display data corresponding to the pitch motion corrupted with additive Gaussian white noise with variance 0.078 (SNR = 5). The asymptotic state is an LCO.

The UF method is applied directly to the noisy data. Because the nonlinearities are expressed only in terms of α and ξ, we consider a reduced form in which the state variable x includes only the pitch angle α, the plunging deflection ξ, their derivatives α' and ξ', and the system parameters. There is no obvious relation between the parameters of the reduced and original system, but because we

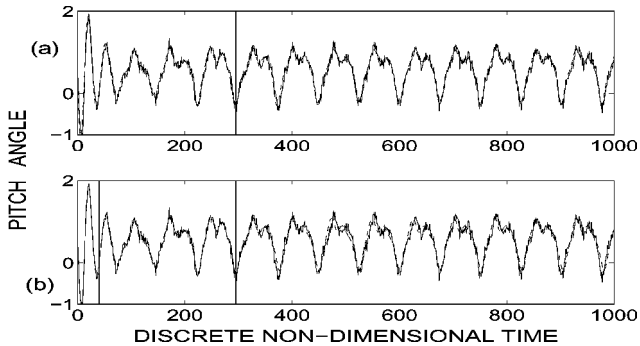

Fig. 2 Simulated LCOs: a) ——, pitch motion and – – –, UF prediction and b) ——, pitch motion and – – –, EXPAR prediction.

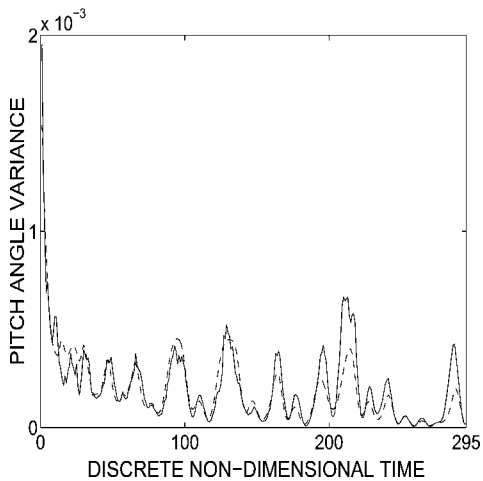

Fig. 3 Performance: ——, Monte Carlo estimated variances and – – –, UF MSE.

are mainly interested in prediction, it is desirable to work with the reduced form.

In order to examine the performances of the UF method, we perform a Monte Carlo simulation to obtain estimates of the true covariance. After tuning the filter, we apply the filter to 50 different sets of data simulated using the clean signal and additive Gaussian white noise with variances 0.078 and 0.25, for α and ξ, respectively. The training set is formed with the first 295 noisy observations plotted in Fig. 2a. The first 295 observations plotted with dashed lines represent the average filtered signal for the pitch motion. In Fig. 3, we present the average mean-square errors (MSE) calculated using the UF, that is, the average of the diagonal elements of the covariance predicted with UF, together with estimations of the true variances using the Monte Carlo simulation. Here the UF is dealing with a continuous piecewise linear function. Despite the fact that this function is not differentiable, the performances of the filter are excellent. Thus, the UF can be regarded as a reliable tool to perform good predictions. Indeed, Fig. 2a indicates excellent agreement between the predictions (dashed lines), starting at $n = 295$, and the simulated noisy signal (solid lines). We observe that even the long-term predictions are very accurate.

The UF method requires additional information regarding the associated aeroelastic system and the nature of the nonlinearities. However, to fit an EXPAR model, we only need the discrete time series. Because the accuracy of the results obtained with the nonlinear time series method is sensitive to the SNR, we first apply a denoising procedure using a translation invariant hard thresholding with the Daubechies orthogonal wavelets.[17] In Fig. 2b, we compare the noisy signals (solid line) with the denoised signals (dashed line), for $n = 1$ to $n = 294$. Using the denoised signal, we fit an EXPAR model with polynomials of degree 3, $\gamma = 11.89$, $p = 20$, and training sets from $n = 40$ to $n = 294$. The predictions (dashed line), for $n = 295$ to $n = 1000$, are also displayed in Fig. 2b.

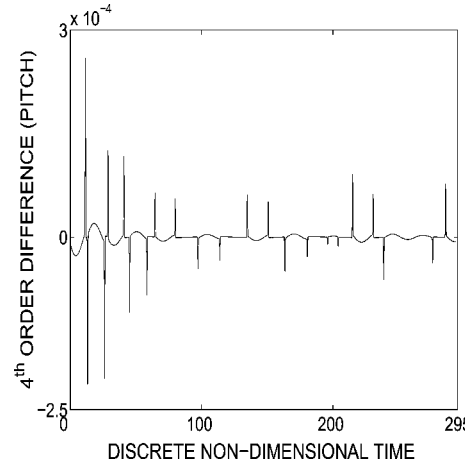

Fig. 4 Fourth-order difference in pitch motion.

The EXPAR models do not require any information about the threshold structure of the freeplay nonlinearity. However, from the study of the fourth-order differences of the simulated aeroelastic signal associated with the noisy observations, we notice periodical changes in the dynamics of the model, as shown in Fig. 4. This is caused by the nondifferentiability of the function $M(\alpha)$ near the switching points. The values corresponding to the peaks shown in Fig. 4 are indeed corresponding to the exact locations of the switching points in the freeplay model, where $\alpha = 0.25$ and $\alpha = 0.75$ in the present case study. Thus, from studying the differences of the simulated signal, we are able to determine whether the nonlinearity is represented by a freeplay model. Moreover, we can also estimate the corresponding freeplay parameters. Robust techniques for finding the threshold structure in the presence of noise are currently being investigated.

To improve our nonlinear predictions, we implement the threshold structure into the nonlinear time series model. Hence, we combine the SETAR with the EXPAR models. Because there are more parameters to be estimated, the sampling step is reduced for the initial time series. The delay parameter $d = 8$ is found by studying the plots of several lagged regressions.[18] An EXPAR model (1) is used for the first region, and EXPAR models (2) with polynomials of degrees 3 and 2, respectively, are fitted for the other two regions. The prediction results are very similar to those shown in Fig. 2b, but the model becomes more complicated.

When the results obtained using the UF (Fig. 2a) are compared, the predictions using nonlinear time series models are less accurate. However, the predicted frequencies and amplitudes of LCOs are in good agreement with the simulated data.

Even though we only report the results in the pitch degree of freedom, the proposed EDMS also provides excellent predictions for the corresponding plunge motions. When the UF method is applied, we obtain accurate predictions for both the pitch and plunge motions and their derivatives.

The EDMS can be used also for predicting divergent signals. To illustrate this for the pitch motion, we generate the noisy signal (solid line) shown in Fig. 5. Because the results obtained using EXPAR models are similar, we present only the predictions using the UF approach.

The training set contains the first 294 observations (solid lines). Looking only at this transient data, it seems that the asymptotic state of the system may be an LCO. However, the EDMS accurately predicts the long-term behavior of this divergent system. The filtered signal (dashed line, from $n = 1$ to $n = 294$) and the predictions (dashed line, from $n = 295$ to $n = 1500$) for the pitch motion are also shown in Fig. 5.

Experimental Data

We illustrate the performance of the EDMS for wind-tunnel experimental data recorded at the Texas A&M University. The data are

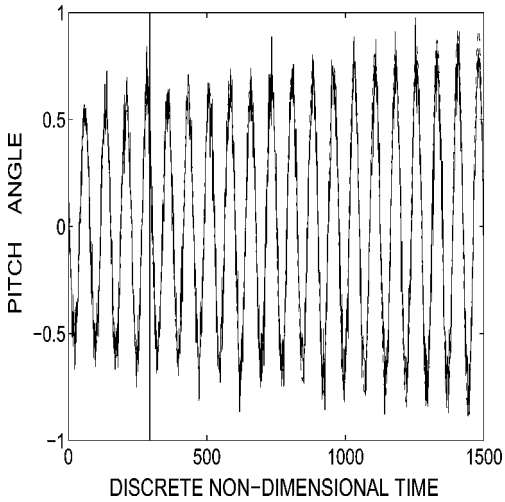

Fig. 5 Divergent signals: ——, unstable oscillations of the pitch displacement and – – –, UF prediction.

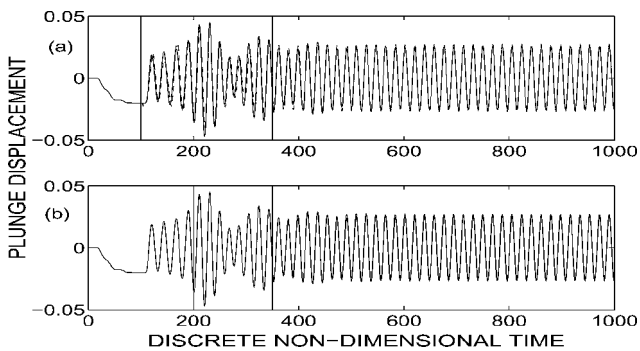

Fig. 6 Experimental LCO: a) ——, plunge motion and – – –, UF prediction and b) ——, plunge motion and – – –, EXPAR prediction.

available at http://aerounix.tamu.edu/aeroel [cited 21 May 2003]. We consider two cases studies, one corresponding to a LCO (data from the file DN04J.dat) and the other corresponding to a steady state (data from the file DN04A.dat). Because the noise effect associated with the observations is not too severe, no denoising procedure is necessary when fitting the EXPAR models. To apply the UF, we consider the state-space form[5] of the following mathematical model, which corresponds to the experimental data:

$$\begin{bmatrix} m & mx_\alpha b \\ mx_\alpha b & I_\alpha \end{bmatrix} \begin{bmatrix} \xi'' \\ \alpha'' \end{bmatrix} + \begin{bmatrix} c_\xi & 0 \\ 0 & c_\alpha \end{bmatrix} \begin{bmatrix} \xi' \\ \alpha' \end{bmatrix} + \begin{bmatrix} k_\xi & 0 \\ 0 & k_\alpha(\alpha) \end{bmatrix} \begin{bmatrix} \xi \\ \alpha \end{bmatrix} = \begin{bmatrix} -L \\ M \end{bmatrix} \tag{29}$$

The term $k_\alpha(\alpha)$ is the nonlinear spring stiffness associated with the pitching motion, and it can be approximated by a polynomial.[5]

The results for the LCO case are shown in Fig. 6 for the plunge motion. In the UF approach, the training set contains data from $n = 100$ to $n = 349$. The measured signal (solid lines) is compared with the filtered (dashed lines, from $n = 100$ to $n = 349$) and predicted signals (dashed lines, from $n = 350$ to $n = 1000$). The results presented in Fig. 6a demonstrate accurate long-term predictions. For the LCO data set, excellent predictions are also obtained using the EXPAR models. The measured (solid lines) and the predicted (dashed lines) signals are shown in Fig. 6b. For the plunge motion, the predictions start again at $n = 350$, and the training set contains only the observations between $n = 200$ and $n = 349$. In the EXPAR model, polynomials of degree 3 are employed with $p = 12$ and $\gamma = 43.1$.

From the first 350 transient observations, the prediction leading to an LCO is not obvious. However, the results presented in Fig. 6 clearly demonstrate that both methods implemented in EDMS are capable of providing excellent long-term predictions for the plunge displacement.

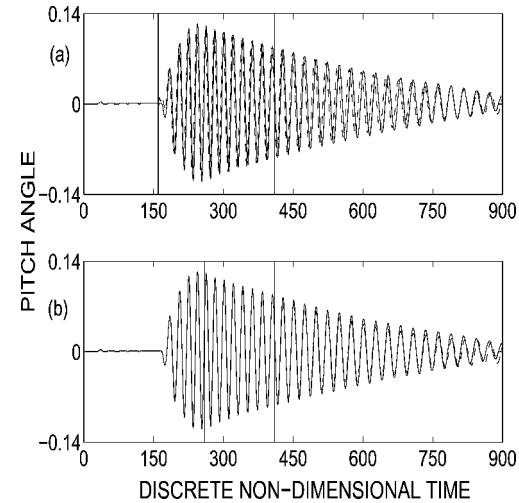

Fig. 7 Experimental damped oscillation: a) ——, pitch motion and – – –, UF prediction and b) ——, pitch motion and – – –, EXPAR prediction.

In Fig. 7, we present the results obtained for the pitch motion when the aeroelastic system exhibits a steady damped oscillation. For the plunge motion, the quality of the prediction is similar, and they are not reported here. In the UF approach, the training set contains the observations from $n = 160$ to $n = 409$. The measured signal (solid lines), the filtered signal (dashed lines, from $n = 160$ to $n = 409$), and the predicted signal (dashed lines, from $n = 410$ to $n = 1000$) are shown in Fig. 7a. For the EXPAR model, the predictions (dashed line) starting at $n = 410$ and the measured signal (solid lines) are compared in Fig. 7b. In this model, polynomials of degree 1 are used with $\gamma = 0.1$ and $p = 2$. The training set contains the observations from $n = 260$ to $n = 409$. Both methods are capable of providing accurate predictions for the damped oscillations.

Conclusions

The illustrative case studies reported in the present paper clearly demonstrate that the proposed expert data mining system can accurately predict the LCO and damped and unstable oscillations.

For experimental aeroelastic data with polynomial restoring forces, and for simulated data corresponding to the cubic spring case, the amplitude-dependent EXPAR models seems to be very appropriate. In these cases, the nonlinear time series model provides long-term predictions of the same accuracy or sometimes even greater accuracy than the UF.

For a freeplay model, the predictions obtained using the UF are more accurate than those obtained with nonlinear time series models. For the present case studies, the UF seems to perform more effective denoising than the wavelet filters. However, the wavelet filters and the time series models do not require any information about the structure of the dynamic system associated with the input data. To implement the UF method, even if no information about the system parameters is given, the specific type of the nonlinearities associated with the aeroelastic system must be known. Thus, for a freeplay model, the extra information seems to be the reason leading to better performance.

The proposed expert data mining system can be considered a useful tool in the study of nonlinear aeroelastic response. Other methods, such as neural networks or the expectation maximization algorithm, can be easily incorporated in the processing module of the expert data mining system. The present investigation also offers the opportunity for using the same approach in other applications, such as flight dynamics and active vibration control systems.

Acknowledgments

This work is supported by the Natural Sciences and Engineering Research Council of Canada. We are grateful to Thomas W. Strganac for giving us the permission to use the experimental data recorded at Texas A&M University. We also thank Liping Liu for providing us with the simulated data and the reviewers for many valuable suggestions.

References

[1]Denegri, C. M., Jr, "Limit-Cycle Oscillation Flight Test Results of a Fighter with External Stores," *Journal of Aircraft*, Vol. 37, No. 5, 2000, pp. 761–769.

[2]Lee, B. H. K., Price, S. J., and Wong, Y. S., "Nonlinear Aeroelastic Analysis of Airfoils: Bifurcation and Chaos," *Progress in Aerospace Sciences*, Vol. 35, No. 3,1999, pp. 205–334.

[3]Tang, D. M., Dowell, E. H., and Virgin, L. N., "Limit Cycle Behavior of an Airfoil with a Control Surface," *Journal of Fluids and Structures*, Vol. 12, No. 7, 1998, pp. 839–858.

[4]Tang, D. M., Henry, J. K., and Dowell, E. H., "Limit-Cycle Oscillations of Delta Wing Models in Low Subsonic Flow," *AIAA Journal*, Vol. 37, No. 11, 1999, pp. 1355–1362.

[5]Ko, J., Strganac, T. W., and Kurdila, A. J., "Stability and Control of a Structurally Nonlinear Aeroelastic System," *Journal of Guidance, Control, and Dynamics*, Vol. 21, No. 5, 1998, pp. 718–725.

[6]Kurdila, A. J., Strganac, T. W., Junkins, J. L., Ko, J., and Akella, M. R., "Nonlinear Control Methods for High-Energy Limit-Cycle Oscillations," *Journal of Guidance, Control, and Dynamics*, Vol. 24, No. 1, 2001, pp. 185–192.

[7]Voitcu, O., and Wong, Y. S., "Neural Network Approach for Nonlinear Aeroelastic Analysis," *Journal of Guidance, Control, and Dynamics*, Vol. 26, No. 1, 2003, pp. 99-105.

[8]Julier, S. J., Uhlmann, J. K., and Durrant-Whyte, H. F., "A New Approach for Filtering Nonlinear Systems," *Proceedings of the American Control Conference*, IEEE, New York, 1995, pp. 1628–1632.

[9]Torii, H., and Matsuzaki, Y., "Flutter Boundary Prediction Based on Nonstationary Data Measurement," *Journal of Aircraft*, Vol. 34, No. 3, 1997, pp. 427–432.

[10]Torii, H., and Matsuzaki, Y., "Flutter Margin Evaluation for Discrete-Time Systems," *Journal of Aircraft*, Vol. 38, No. 1, 2001, pp. 42–47.

[11]Andrighettoni, M., and Mantegazza, P., "Multi-Input/Multi-Output Adaptive Active Flutter Suppression for a Wing Model," *Journal of Aircraft*, Vol. 35, No. 3, 1998, pp. 462–469.

[12]Dimitriadis, G., and Cooper, J. E., "Flutter Prediction from Flight Flutter Test Data," *Journal of Aircraft*, Vol. 38, No. 2, 2001, pp. 355–367.

[13]Lyons, M. G., Vepa, R., McIntosh, S. C., and DeBra, D. B., "Control Law Synthesis and Sensor Design for Active Flutter Suppression," *Proceedings of the AIAA Guidance and Control Conference*, AIAA, New York, 1973, pp. 1–29.

[14]Block, J. J., and Strganac, T. W., "Applied Active Control for a Nonlinear Aeroelastic Structure," *Journal of Guidance, Control, and Dynamics*, Vol. 21, No. 6, 1998, pp. 838–845.

[15]Julier, S. J., and Uhlmann, J. K., "A New Extension of the Kalman Filter to Nonlinear Systems," *Proceedings of AeroSense: The 11th International Symposium on Aerospace/Defense Sensing, Simulation and Controls*, SPIE, Bellingham, WA, 1997.

[16]Mallat, S., *A Wavelet Tour of Signal Processing*, Academic Press, London, 1999.

[17]Daubechies, I., *Ten Lectures on Wavelets*, Society for Industrial and Applied Mathematics, Philadelphia, 1992.

[18]Tong, H., *Nonlinear Time Series*, Oxford Univ. Press, Oxford, 1990.

[19]Haggan, V., and Ozaki, T., "Modeling Nonlinear Random Vibrations Using an Amplitude-Dependent Autoregressive Time Series Model," *Biometrika*, Vol. 68, No. 1, 1981, pp. 189–196.

[20]Ozaki, T., "The Statistical Analysis of Perturbed Limit Cycle Processes Using Nonlinear Time Series Models," *Journal of Time Series Analysis*, Vol. 3, No. 1, 1982, pp. 29–41.

[21]Tong, H., and Lim, K. S., "Threshold Autoregression, Limit Cycles and Cyclical Data," *Journal of the Royal Statistical Society*, Vol. 42, No. 3, 1980, pp. 245–292.

[22]Popescu, C. A., and Wong, Y. S., "The Unscented and Extended Kalman Filter for Systems with Polynomial Restoring Forces," AIAA Paper 2003-1410, April 2003.